Time-Resolved Infrared Spectroscopy of $K_3Ta_3B_2O_{12}$ Photocatalysts for Water Splitting

Toshitatsu Ikeda,[†] Satoru Fujiyoshi,[†,§] Hideki Kato,[‡] Akihiko Kudo,[‡,§] and Hiroshi Onishi*[,†]

Department of Chemistry, University of Kobe, 1-1 Rokkodai-cho, Nada-ku, Kobe 657-8501, Japan, Department of Chemistry, Science University of Tokyo, 1-3 Kagurazaka, Shinjuku-ku, Tokyo, 162-8601, Japan, and Core Research for Evolutional Science and Technology, Japan Science and Technology Agency (CREST-JST), 4-1-8 Honcho, Kawaguchi-shi, Saitama 332-0012, Japan

Received: December 27, 2005; In Final Form: February 24, 2006

Electrons photoexcited in $K_3Ta_3B_2O_{12}$, an efficient photocatalyst for the water-splitting reaction driven by ultraviolet light, were observed using time-resolved IR absorption spectroscopy with microsecond resolution. When the catalyst was irradiated with 266 nm light pulses, a structureless absorption appeared at 3000−1500 cm^{-1}. The absorption was assigned to the optical transition of electrons that were band gap-excited and then trapped in mid-gap states. The absorbance decayed with a time delay because of the electron−hole recombination. The rate of recombination in an argon atmosphere was sensitive to the composition of the starting material used in the catalyst preparation. The electron decay was accelerated by exposing the catalyst to water vapor. The degree of acceleration was qualitatively correlated with the H_2 production rate observed during steady-state light irradiation.

1. Introduction

Photocatalytic hydrogen production from water is one of the more promising approaches to solar energy conversion. Intense effort has been devoted to the splitting of water with visible light irradiation.[1−4] Water splitting with ultraviolet (UV) light is now possible on a number of mixed metal oxides, including TiO_2,[5] $SrTiO_3$,[6] $K_4Nb_6O_{17}$,[7] and MIn_2O_4 (M = Ca, Sr).[8] A small amount of a second compound is often added to these oxides to improve the rate of H_2 production. Platinum,[9] Rh,[10] and NiO[5−7] are typical additives (cocatalysts). Certain tantalates such as $K_3Ta_3Si_2O_{13}$,[11] $LiTaO_3$, $NaTaO_3$, $KTaO_3$,[12,13] $Sr_2Ta_2O_7$,[14] and $K_2LnTa_5O_{15}$[15] provide active H_2 production without a cocatalyst. $K_3Ta_3Si_2O_{13}$ has a particularly interesting structure; TaO_6 octahedra corner shared with each other provide straight pillars parallel to the *c* axis of the crystal, and the TaO_6 pillars are linked by SiO_4 tetrahedral units.[16] Photoexcited electrons and holes are proposed to be mobile along the corner-shared octahedra when the metal−oxygen−metal angle is close to 180°.[17] This requirement is fulfilled in $K_3Ta_3Si_2O_{13}$.

The dynamics of electrons photoexcited in $K_3Ta_3B_2O_{12}$, another pillared tantalate, are examined in the present study. The SiO_4 tetrahedra in $K_3Ta_3Si_2O_{13}$ are replaced by planar BO_3 units as shown in Figure 1.[18] This boron-containing tantalate, the band gap of which was experimentally determined to be 4.2 eV, is highly active for water splitting in the absence of a cocatalyst. Two millimoles of H_2 and 1 mmol of O_2 were produced per hour when an aqueous suspension containing 1.0 g of catalyst was irradiated with a 450 W high-pressure Hg lamp.[19] By substituting boron for silicon, the rate of H_2 production was improved by a factor of 50. The electron dynamics in the active tantalate are observed with time-resolved infrared absorption (TRIR) spectroscopy, which is a powerful method for the investigation of the dynamics of electrons and holes.[20,21] The decay of the electron population because of electron−hole recombination and a water-induced surface reaction was traced in the microsecond time domain. The rate of H_2 production, which was sensitive to the boron content, is discussed on the basis of the observed electron dynamics.

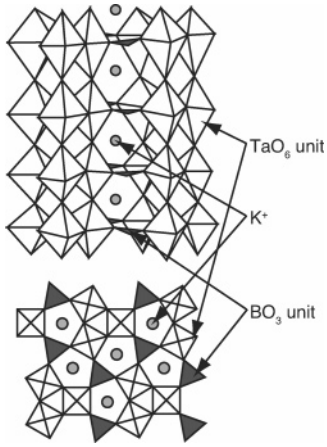

Figure 1. Structure of $K_3Ta_3B_2O_{12}$.

2. Experimental Section

A home-built spectrometer (Figure 2)[22] was used. The catalyst was placed in a gas cell and was irradiated by 266 nm light pulses from the fourth harmonic of a Q-switched Nd:YAG laser source (LOTIS TII, LS-2139). The pulse energy, time width, and repetition frequency were 0.4 mJ, 20 ns, and 100 Hz, respectively. Irradiation with more intense pulses induced thermal emission of IR light from catalyst particles heated by the nonradiative recombination of electron−hole pairs. The diameter of the irradiated spot was 6 mm. Continuous-wave IR light from a ceramic globar source passing through the catalyst was dispersed in a grating monochromator with a 25 cm focal length. A MCT detector received the monochromatized light.

* To whom correspondence should be addressed. E-mail: oni@kobe-u.ac.jp.
[†] Kobe University.
[‡] Science University of Tokyo.
[§] CREST.

10.1021/jp057536x CCC: $30.25
Published on Web 03/25/2006

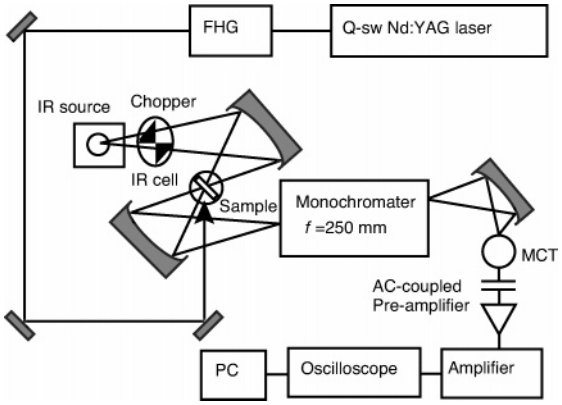

Figure 2. Diagram of the time-resolved infrared spectrometer.

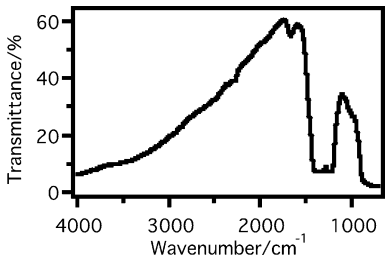

Figure 3. Steady-state IR transmittance spectrum of catalyst **A** observed in the dark.

Gratings of 300 and 150 grooves/mm were used for the 3000−2000 and 2000−1000 cm^{-1} measurements, respectively. The MCT signal voltage was amplified in AC-coupled amplifiers (NF circuit, NF 5307; Stanford Research Systems, SR560). Absorbance changes as small as 10^{-5} were traced as a function of the time delay from the UV pump pulse. Five thousand responses were required to make a trace at one wavenumber. To improve the signal-to-noise ratio of the absorbance change, the repetition rate of the pump light pulses was increased from 10 Hz[22] to 100 Hz in the present study. The steady-state IR absorption spectrum of the catalyst was observed with an FT-IR spectrometer (JASCO, FT/IR 610) at a spectral resolution of 4 cm^{-1}.

$K_3Ta_3B_2O_{12}$ was synthesized by calcination of a mixture of K_2CO_3, Ta_2O_5, and H_3BO_3 in air at 1173 K for 10 h.[19] The catalytic activity was sensitive to the boron content in the starting material. Catalysts prepared with a 10% excess boron (catalyst **A**) and those prepared with a 20% excess boron (catalyst **B**) were compared in the present study. The potassium content in the mixture was fixed at 5% excess versus the stoichiometric amount. Scanning electron microscopy (SEM) revealed that the particle size of catalyst **A** was similar to that of catalyst **B**. Pillars were 0.2−0.3 μm in width and 0.5−0.8 μm in length. The absorption edge of the calcined catalysts (both **A** and **B)** was 295 nm in wavelength.[19] The catalyst was loaded on a CaF_2 plate with a density of 3 mg cm^{-2} and placed in a gas cell. The catalyst was suspended in distilled water, deposited onto a CaF_2 plate with a pipet, and dried in air.

3. Results and Discussion

3.1. Steady-State Spectrum in the Dark. Figure 3 shows the transmittance spectrum of catalyst **A**. The transmittance of IR light decreased with increasing wavenumber in the range of 4000−1500 cm^{-1}. The cutoff observed around 900 cm^{-1} was the result of the light absorption of the CaF_2 plate. This monotonic spectrum is ascribed to light scattering by catalyst particles rather than absorption. Another feature of the spectrum is an intense depression at 1500−1100 cm^{-1}. This abrupt feature is presumably caused by the absorption by lattice vibrations of the boron-containing oxide. Lattice vibrations related to boron atoms incorporated are expected at high wavenumbers.[23]

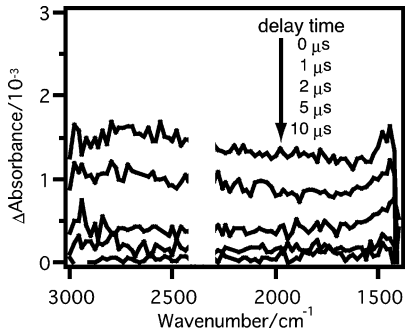

Figure 4. Time-resolved IR absorption spectra of catalyst **A** irradiated by a 266 nm, 20 ns, 0.4 mJ light pulse. The catalyst was irradiated in 10 Torr of argon gas.

3.2. Transient Absorption Caused by UV Light Pulse. Figure 4 shows the transient absorption spectra of **A**. The catalyst was placed in the gas cell filled with 10 Torr argon gas and irradiated with the UV pulses. The argon environment was effective at minimizing the thermal emission of mid-IR light. The heat produced in the irradiated catalyst particles is released to the gas environment. The spectra observed at different time delays exhibited a structureless feature. The absolute intensity decreased with increasing time delay, leaving the shape of spectrum unchanged. The transient response was observed at 3000−1400 cm^{-1}. The scattering caused by catalyst particles determined the high-wavenumber end of the observable range, whereas the absorption caused by the lattice vibration limited the low-wavenumber end. The absorption by CO_2 in the light path made it difficult to trace the transient response at 2400−2300 cm^{-1}.

The transient spectrum exhibited a structureless feature, a broad peak around 3000 cm^{-1}, and a monotonic increase with decreasing wavenumber at 1650−1450 cm^{-1}. The whole profile is different from the steady-state spectrum presented in Figure 3 and is hence assigned to light absorption by the UV-excited catalyst, not to light scattering caused by the UV irradiation. The UV-induced IR absorption observed on TiO_2[22] and $NaTaO_3$[24] increased monotonically with decreasing wavenumber and was assigned to the absorption by free electrons in the conduction band. Infrared absorption by free electrons is characterized by a monotonic spectrum which increases as ν^{-p} (ν is the wavenumber and p ranges from 1.5 to 3.5).[25] The spectrum shown in Figure 4 deviates from this formula. The optical transition of electrons that are band gap-excited and then trapped in mid-gap states is proposed instead. The electrons in the mid-gap states are excited to the conduction band by IR light absorption.[26] When trap states of different depths are present, the optical absorption spectrum can be flat and structureless.

To support this assignment to electrons, the transient IR absorption was observed in the presence of oxygen gas (an electron scavenger) or methanol gas (a hole scavenger). The absorbance at 2000 cm^{-1} was traced as a function of the time delay and plotted in Figure 5. The decay of absorbance observed in the argon atmosphere reflected the electron−hole recombination in the catalyst particles. When the catalyst was exposed to 10 Torr O_2 gas, the decay was accelerated at time delays of 5

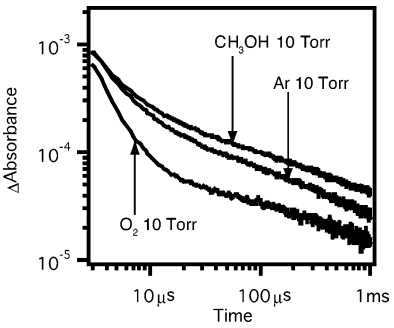

Figure 5. Temporal profile of IR absorbance at 2000 cm^{-1}. Catalyst **A** was irradiated with the pump light pulses of 266 nm and 0.4 mJ. The transient absorbance at 2000 cm^{-1} was traced as a function of time delay in 10 Torr of argon gas, 10 Torr of oxygen gas, or 10 Torr of methanol vapor.

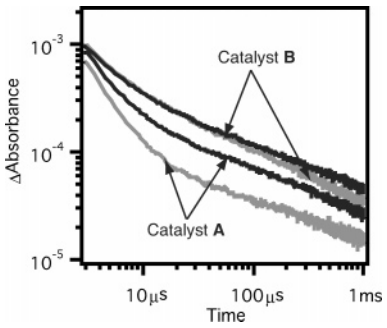

Figure 6. Temporal profile of IR absorbance of catalyst **A** and catalyst **B**. Response curves were observed in 10 Torr of argon gas (black line) and in 10 Torr of water vapor (gray line). The pump light pulses of 266 nm and 0.4 mJ were used, and the transient absorbance at 2000 cm^{-1} was traced as a function of time delay.

μs and later. The accelerated decay is attributed to electron capture by O_2

$$O_2\,(g) + e^- \rightarrow O_2^-\,(a) \qquad (1)$$

where g and a represent the gas and adsorbed phases, respectively. An equal efficiency of cooling is expected with argon and oxygen atmospheres of the same pressure. In our previous studies, exposure to an O_2 atmosphere induced an acceleration of the electron decay at 1 μs on $NaTaO_3$[24] and at 10 μs on TiO_2 (P-25).[27] The acceleration occurred at shorter time delays on $NaTaO_3$ and on $K_3Ta_3B_2O_{12}$ than on TiO_2. This is consistent with the more negative potential of electrons excited in the conduction band of the two tantalates. The large band gaps (4.1 eV for $NaTaO_3$ and 4.2 eV for $K_3Ta_3B_2O_{12}$) imply conduction bands that are more negative by 1 eV than that of TiO_2. The valence bands of the three oxides are composed of O 2p orbitals and are assumed to lie at a common redox potential.

On the other hand, the recombination was retarded by exposure to 10 Torr of CH_3OH vapor, as shown in Figure 5. CH_3OH-derived adsorbates capture holes

$$CH_3O^-\,(a) + h^- \rightarrow CH_3O^{\bullet}\,(a) \qquad (2)$$

and compete with electron−hole recombination. CH_3OH-induced retardation was apparent at 10 μs. The recombination was partially retarded on the $K_3Ta_3B_2O_{12}$ catalyst, while it was totally suspended in TiO_2 exposed to CH_3OH vapor of the same pressure. This suggests that the holes generated in $K_3Ta_3B_2O_{12}$ are less probable to attack the scavengers absorbed at the surface. The large size of the tantalate particles may be a reason for the restricted probability of hole-induced reactions at the surface.

The absorbance decay being accelerated with O_2 exposure and retarded with CH_3OH exposure supports our assignment of the IR absorption to electrons. Hence, we assume that the absorbance at 2000 cm^{-1} represents the number of band gap-excited electrons. The effect of catalyst modification is examined in the following section based on this assumption.

3.3. Boron Content in the Starting Material. The amount of H_3BO_3 in the starting mixture controls the activity of the calcined catalyst. The rate of H_2 production on 1.0 g of catalyst **A** (prepared with a 10% excess of boron) was 2.1 mmol/h and decreased to 0.5 mmol/h on the same amount of catalyst **B** (prepared with a 20% excess of boron).[28] The electron−hole recombination in **A** was compared to that of **B**. Figure 6 presents the absorbance decay of the two catalysts observed in the 10 Torr argon atmosphere. Catalyst **B** exhibited larger absorbance at all time delays, which suggests more electrons not yet recombined. This is presumably because the excess boron in the starting mixture of **B** compensated for the sublimated loss in the calcination. Boron-deficient portions of the calcined catalysts can be poorly ordered and may contain recombination centers. In $NaTaO_3$, the rate of electron−hole recombination was sensitive to the Na content, and this was interpreted in a similar manner.[24] Catalysts **A** and **B** contained particles of comparable size as mentioned in the Experimental Section. A major contribution of the different surface areas is less probable because of the decay kinetics observed on the two.

It is well-known that redox reactions at a photocatalyst surface compete with the electron−hole recombination in the bulk. Figure 6 shows more electrons available in **B** than in **A**. The rate of H_2 production was, however, four times smaller on **B** than on **A**. Thus, the amount of electrons was not related to the reaction rate. This is different from the situation observed for a series of $NaTaO_3$ catalysts.[24] On that compound, the rate of H_2 production was positively correlated with the electron number observed with IR absorption.

The negative relationship is interpreted on the basis of highly efficient electron transfer at the surface of **A**. This is supported by the decay curves observed in 10 Torr of water vapor (Figure 6). On **A**, the decay was accelerated at 5 μs when compared with the curve of the same catalyst observed in argon. This acceleration is attributed to electron transfer from the catalyst to water-induced adsorbates, as has been proposed on Pt/TiO_2[27] and $NaTaO_3$.[24] On **B**, the electron decay was only slightly accelerated at 100 μs in the water vapor. The restricted acceleration is consistent with the reduced rate of H_2 production. As mentioned in the Introduction, $K_3Ta_3B_2O_{12}$ is highly active for water splitting without a cocatalyst. Particular sites that allow electrons to attack the water-induced adsorbates are expected on the surface of **A**. The number of surface sites efficient for H_2 production is reduced on **B**, even though the bulk stoichiometry is favorable to minimize the rate of recombination. This consideration suggests that the reaction rate of **B** can be improved with an appropriate cocatalyst. The excess boron in the starting material of **B** may have been transformed to KBO_3 in the calcination and may have encapsulated the $K_3Ta_3B_2O_{12}$ particles.

The other feature to be considered in Figure 6 is the time delay at which the water-induced acceleration was apparent: 5 μs on **A** and 100 μs on **B**. The time delays represent the characteristic time of electron transfer at the catalyst surface. The short delay on **A** suggests an efficient electron transfer, which is consistent with the active H_2 production. Actually, the characteristic time of electron transfer, which was deduced in

our time-resolved IR studies, correlates well with the H_2 production rate. La-doped $NaTaO_3$ with NiO cocatalyst,[13] $K_3Ta_3B_2O_{12}$ (catalyst **A**), and Pt/TiO_2[9] produced 20 mmol, 2 mmol and 30 μmol of H_2/h, respectively, when irradiated with a similar flux of UV light. The electron-transfer times of the three catalysts were 1,[24] 5, and 200 μs,[27] respectively, reproducing the order of the H_2 production rates.

4. Conclusions

The electron dynamics in $K_3Ta_3B_2O_{12}$ photocatalysts for water splitting were traced using time-resolved IR absorption spectroscopy. When the catalyst was irradiated with 266 nm light pulses, a structureless absorption appeared at 3000−1500 cm^{-1}, which was assigned to absorption by electrons UV-excited and then trapped in mid-gap states. The electron−hole recombination observed in the argon atmosphere was sensitive to the boron content in the starting material in catalyst preparation. The decay of the electrons was accelerated by exposing the catalyst to water vapor. The contribution of the electron-transfer reaction was identified at a time delay of 5 μs. The degree of acceleration was qualitatively correlated with the rate of H_2 production observed in steady-state UV irradiation.

Acknowledgment. The authors thank Toshiyasu Kurihara for preparing the catalysts. This work was supported by the Core Research for Evolutional Science and Technology (CREST) Program of the Japan Science and Technology Agency (JST) and a Grant-in-Aid (14050090) from the Ministry of Education, Science, Sports, and Culture of Japan.

References and Notes

(1) Kudo, A.; Kato, H.; Tsuji, I. *Chem. Lett.* **2004**, 1534.
(2) Domen, K.; Kondo, J. N.; Hara, M.; Takata, T. *Bull. Chem. Soc. Jpn.* **2000**, *137*, 1307.
(3) Kudo, A. *Catal. Surv. Asia* **2003**, *7*, 31.
(4) Kato, H.; Kudo, A. *Catal. Today* **2003**, *78*, 561.
(5) Kudo, A.; Domen, K.; Maruya, K.; Onishi, T. *Chem. Phys. Lett.* **1987**, *133*, 517.
(6) Domen, K.; Kudo, A.; Onishi, T. *J. Catal.* **1986**, *102*, 92.
(7) Kudo, A.; Sayama, K.; Tanaka, A.; Asakura, K.; Domen, K.; Maruya, K.; Onishi, T. *J. Catal.* **1989**, *120*, 337.
(8) Sato, J.; Saito, S.; Nishiyama, H.; Inoue, Y. *J. Phys. Chem. B* **2001**, *105*, 6061.
(9) Tabata, S.; Nishida, H.; Masaki, Y.; Tabata, K. *Catal. Lett.* **1995**, *34*, 245.
(10) Yamaguchi, K.; Sato, S. *J. Chem. Soc., Faraday Trans. 1* **1985**, *81*, 1237.
(11) Kudo, A.; Kato, H. *Chem. Lett.* **1997**, 867.
(12) Kato, H.; Kudo, A. *J. Phys. Chem. B* **2001**, *105*, 4285.
(13) Kato, H.; Asakura, K.; Kudo, A. *J. Am. Chem. Soc.* **2003**, *125*, 3082.
(14) Kudo, A.; Kato, H.; Nakagawa, S. *J. Phys. Chem. B* **2000**, *104*, 571.
(15) Kudo, A.; Okutomi, H.; Kato, H. *Chem. Lett.* **2000**, 1212.
(16) Choisnet, J.; Nguyen, N.; Groult, D.; Raveau, B. *Mat. Res. Bull.* **1976**, *11*, 887.
(17) Alacon, J.; Blasse, G. *J. Phys. Chem. Solids* **1992**, *53*, 677.
(18) Abrahams, S. C.; Zyontz, L. E.; Bernstein, J. L.; Remeika, J. P.; Cooper, A. S. *J. Chem. Phys.* **1981**, *75*, 5456.
(19) Kurihara, T.; Okutomi, H.; Miseki, Y.; Kato, H.; Kudo, A. *Chem. Lett.* **2006**, *35*, 274.
(20) Yamakata, A.; Ishibashi, T.; Onishi, H. *J. Mol. Catal. A* **2003**, *199*, 85.
(21) Yamakata, A.; Ishibashi, T.; Takeshita, K.; Onishi, H. *Topics Catal.* **2005**, *35*, 211.
(22) Yamakata, A.; Ishibashi, T.; Onishi, H. *Chem. Phys. Lett.* **2001**, *333*, 271.
(23) Guo, Q.; Xie, Y.; Yi, C.; Zhu, L.; Gao, P. *J. Solid State Chem.* **2005**, *178*, 1925.
(24) Yamakata, A.; Ishibashi, T.; Kato, H.; Kudo, A.; Onishi, H. *J. Phys. Chem. B* **2003**, *107*, 14383.
(25) Pankove, J. *Optical Processes in Semiconductors*; Dover: New York, 1975.
(26) Warren, D. S.; McQuillan, A. J. *J. Phys. Chem. B* **2004**, *108*, 19373.
(27) Yamakata, A.; Ishibashi, T.; Onishi, H. *J. Phys. Chem. B* **2001**, *105*, 7258.
(28) The rates of H_2 production are slightly different from those reported in ref 19: 1.8 mmol/h for catalyst **A** and 1.1 mmol/h for catalyst **B**. This is because separately calcined catalysts exhibited limited fluctuation in the rate.